Macromolecules
ARTICLE

Macromolecules **2010**, *43*, 9473–9479 **9473**
DOI: 10.1021/ma102043d

Confinement Effects on Cross-Linking within Electrostatic Layer-by-Layer Assemblies Containing Poly(allylamine hydrochloride) and Poly(acrylic acid)

Woo-Sik Jang,[†] Anne T. Jensen,[‡] and Jodie L. Lutkenhaus*[,⊥,§]

[†]*Department of Physics, Yale University, New Haven, Connecticut 06511, United States,* [‡]*Department of Chemical Engineering, University of Connecticut, Storrs, Connecticut 06269, United States, and* [§]*Department of Chemical Engineering, Yale University, New Haven, Connecticut 06511, United States.* [⊥] *Present address: Artie McFerrin Department of Chemical Engineering at Texas A&M University, College Station, TX*

Received September 2, 2010; Revised Manuscript Received October 18, 2010

ABSTRACT: Thermal cross-linking is widely used to impart stability or improved mechanical properties to layer-by-layer (LbL) assemblies. However, the kinetics of thermal cross-linking within LbL films is not well understood. Furthermore, because LbL films are generally ultrathin (< 100 nm), the influence of confinement on cross-linking kinetics is potentially substantial. Using temperature-controlled ellipsometry, differential scanning calorimetry, and thermal gravimetric analysis, we are able to accurately track amide cross-linking within poly(allylamine hydrochloride)/poly(acrylic acid) LbL films. The rate of amidation is strongly influenced by film thickness and surface chemistry, which indicates that the observed "confinement effects" are primarily related to the catalytic contribution of hydroxyl groups present on the substrate's surface. The analytical techniques presented herein highlight new ways to access thermochemical information within ultrathin LbL assemblies.

Introduction

Layer-by-layer (LbL) assemblies have attracted increasing attention in various research fields such as drug delivery,[1−4] biomaterials,[5] antifouling,[6,7] polymer electrolytes,[8−10] fuel cells,[11−13] batteries,[14,15] solar cells,[16,17] thin film transistors,[18,19] thin film capacitors,[20] and nanofluidic applications[21] to improve the performance or to imbed a special function into a system. The LbL assembly technique is the alternate exposure of a substrate to dilute aqueous solutions of oppositely charged (or hydrogen bonding) species[22−24] and is a powerful means to create polymeric nanostructures and thin film coatings. However, material properties of LbL assemblies are challenging to characterize because the films are generally thin and because the supporting substrate is far more massive than the film itself. Furthermore, many LbL assemblies—being made with just a few cycles of deposition—are so thin (< 100 nm) that the influence of confinement on the material properties cannot be ignored. Indeed, characterizing the thermal properties of thin LbL films was cited as a major challenge in a recent review.[25]

The influence of confinement on neutral polymers has been actively studied for over 10 years,[26−28] and LbL assemblies comprised of polyelectrolytes may show analogous effects. Examples of confined polymers at small size scales (generally < 100 nm) include ultrathin films and polymer nanowires. Thermochemical properties such as glass transition temperature (T_g),[29] melting temperature (T_m),[30] and curing temperature (T_{cure})[31] can each vary with thickness. Some "confinement effects" may arise from altered chain structure relative to a substrate[32] and stiffening of chains.[33] For example, Keddie et al.[34] and Kim et al.[35] reported a T_g depression for ultrathin poly(styrene) (PS) films, which was attributed to enhanced segmental mobility. In contrast, other researchers observed little variation of material properties in thin films.[36,37] The behavior of ultrathin neutral polymer films, though actively explored, is not completely understood.

On the other hand, a recent body of work indicates that the kinetics of curing or cross-linking of polymers confined within controlled pore glasses (CPGs) is dependent on pore diameter. Simon et al. reported that the rate of cure of bisphenol M dicyanate ester accelerated with decreasing pore diameter.[31,38,39] The enhanced reactivity and lower curing temperature was attributed to an increased number of collisions between monomers in the vicinity of the substrate. In contrast, Amanuel and Malhotra reported that the curing temperature of phenolic resin in porous silica increased with decreasing pore diameter.[40] The higher curing temperatures were attributed to a loss of entropy induced by physical confinement; to compensate, curing temperature increased. These conflicting reports highlight that the curing behavior of polymers in confined geometries may be dependent on many factors such as supporting substrate, type of polymer, and surface treatment, apart from just film thickness or pore diameter.

Layer-by-layer systems are also known to undergo thermal curing or cross-linking, and this behavior has been exploited to produce robust, stable coatings.[41] Recently, we reported on the thermochemical behavior of bulk free-standing poly(allylamine hydrochloride)/poly(acrylic acid) (PAH/PAA) LbL assemblies characterized using modulated differential scanning calorimetry (MDSC), thermal gravimetric analysis (TGA), and Fourier transform infrared (FTIR) spectroscopy.[42] Whereas homopolymers PAH and PAA each have well-defined glass transition temperatures, PAH/PAA LbL assemblies possessed no apparent glass transition. Instead, the LbL assemblies underwent curing via anhydride formation (∼100 °C) and amidation (∼250 °C) upon heating. Given the previous work, we hypothesize that curing within the LbL assembly may be influenced by film

*Corresponding author. E-mail: jodie.lutkenhaus@che.tamu.edu.

Published on Web 10/29/2010

thickness or number of layer pairs. However, curing is difficult to characterize in ultrathin LbL assemblies because isolation from their substrate is exceedingly difficult.

In the present work, we elucidate how confinement influences curing within PAH/PAA LbL assemblies using conventional analytical techniques that are unconventionally applied to ultrathin LbL assemblies. Fluctuations in dry film thickness were monitored using temperature-controlled ellipsometry, curing kinetics were examined using differential scanning calorimetry (DSC), and changes in film mass were observed using TGA. Results indicate that all techniques can adequately track curing kinetics in ultrathin LbL films and that amidation curing temperature is highly dependent on thickness and substrate surface chemistry. Furthermore, the effect of confinement on amidation curing within ultrathin LbL assemblies may be attributed simply to the catalytic contribution of the substrate. On the other hand, the effects of confinement on anhydride formation were uncertain. The analytical techniques presented are applicable to other LbL systems and provide new opportunities for thermal characterization of ultrathin LbL assemblies.

Experimental Section

Materials. Poly(allylamine hydrochloride) (PAH, 15 000 g/mol, Sigma-Aldrich) and poly(acrylic acid) (PAA, 50 000 g/mol, Polysciences) were dissolved in 18.2 MΩ water (Milli-Q, Millipore) at a concentration of 20 mM based on monomer unit weight and stirred for more than 12 h. The pH of cationic PAH solution was adjusted to 7.5, and that of anionic PAA solution was adjusted to 3.5 using NaOH and HCl. Only one set of pH conditions were examined here because prior work[42] indicated that the cross-linking of PAH/PAA LbL films proceeded similarly regardless of assembly pH. The preceding pH values were chosen because these conditions have been shown to yield LbL assemblies with thick bilayers,[43] which decreases the number of cycles required to reach a desired film thickness. Silicon wafers (University Wafers) were used as substrates for LbL assembly for ellipsometry experiments. Silicon wafers were cleaned with piranha solution (3:1 sulfuric acid to hydrogen peroxide) prior to LbL assembly. *Caution: piranha solution is extremely corrosive, and proper precautions must be taken.* In some cases, the surface of the silicon wafer was modified using hexamethyldisilazane (HMDS, Sigma) following a published procedure.[44] Briefly, a silicon wafer was immersed in boiling nitric acid for 10 h, rinsed, and oven-dried. Then, the wafer was immersed in HMDS at 55 °C for 20 h, rinsed using chloroform, and then dried under vacuum. Commercial anodic aluminum oxide (AAO) membranes (Whatman International) of 200 nm pore diameter were used as substrates for LbL assembly for DSC and TGA experiments. AAO membranes were rinsed with ethanol and 18.2 MΩ water prior to LbL assembly.

LbL Assembly Fabrication. Substrates (silicon wafer or AAO membrane) were plasma treated immediately before LbL assembly and initially dipped in cationic PAH solution for 15 min, followed by 2, 1, and 1 min of successive rinsing steps in 18.2 MΩ water. The same procedure was then followed by exposure to anionic PAA solution and rinsing as before to yield a "layer pair". The samples were dried under vacuum for more than 12 h prior to characterization.

Characterization. Film thickness was monitored using a single-wavelength (λ = 632.8 nm) ellipsometer (Angstrom Advanced). The incident angle was 65°. Thickness was calculated using PhE-101 commercial software (Angstrom Advanced). A programmed heating rate (3 °C/min) was applied to the sample using a Linkam TMS 94 heating stage in ambient air. Figure 1 depicts the experimental apparatus for temperature-controlled ellipsometry. The temperature of the heater and sample were assumed to be identical, as estimated in the Supporting Information. Cross-linking temperatures were calculated from a minimum of three measurements, and the standard deviation was taken as the error.

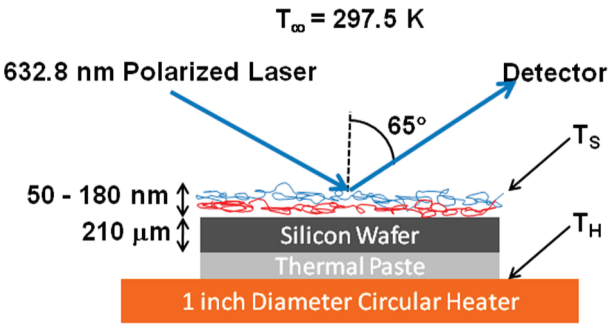

Figure 1. Schematic of the ellipsometer, heating stage, and LbL sample. T_∞ is the ambient temperature, T_S is the sample's surface temperature, and T_H is the hot stage temperature. Here, it is assumed that $T_S \approx T_H$ (see Supporting Information).

DSC (Q200, TA Instruments) samples were dried overnight at room temperature under vacuum prior to testing. 5−10 mg of LbL-coated AAO membranes was crushed and placed into T_{zero} aluminum pans and T_{zero} hermetic lids with pinholes (TA Instruments). Samples were held isothermally at 40 °C under nitrogen for 60 min prior to initializing DSC testing. Then, samples were heated at 3 °C/min, 5 °C/min, or 10 °C/min to 170 °C and held isothermally for 3 min. Samples were then cooled to back to 40 °C using the previous rate and held isothermally for 3 min. In a second cycle, samples were subsequently heated to 300 °C at the same rate, held isothermally for 3 min, and then cooled at the same rate to 40 °C. Two cycles were performed to separately observe the two cross-linking events, which would otherwise overlap. The DSC thermograms were plotted with exotherm down, and data were analyzed using TA Universal Analysis software.

Prior to TGA testing (Q50, TA Instruments), samples were held under vacuum overnight. About 9 mg of LbL-coated AAO membranes was crushed and loaded into a platinum pan. Samples were held isothermally under nitrogen at 40 °C for 60 min to eliminate loosely bound water. Samples were then heated at a rate of 3 °C/min to 170 °C, held isothermally for 3 min, and then cooled to 40 °C at the same rate. Then, samples were held isothermally for 3 min, heated once again at 3 °C/min to 300 °C, and held isothermally for 3 min. TGA thermograms were analyzed using TA Universal Analysis software.

Previous work indicates that the thermal decomposition of both homopolymers PAA and PAH begin to thermally decompose above 250 °C, where PAA undergoes decarboxylation and PAH loses the pendant amine group.[45,46] Amidation of PAH with PAA slows the decomposition rate of PAH/PAA LbL assemblies between 250 and 300 °C;[42] here, the presence of decomposition, typified by large endotherms in DSC thermograms, was not observed. Therefore, thermal decomposition was neglected in our analysis for temperatures below 300 °C.

Results

PAH/PAA LbL assemblies of varying thickness (i.e., number of layer pairs) were first investigated using temperature-controlled ellipsometry with the aim of monitoring changes in film thickness as a result of cross-linking within the film. DSC and TGA were performed on analogous samples to examine the thermal properties of the LbL assemblies and mass lost during the cross-linking reactions. If cross-linking occurs, then film thickness and mass are both expected to decrease at a given cross-linking temperature, which, in turn, may be influenced by initial film thickness.

The real-time film thickness of 5, 6, and 8 layer pairs (LP) of PAH/PAA LbL assemblies on silicon wafer was monitored using temperature-controlled ellipsometry (Figure 2). The initial film thicknesses of the 5, 6, and 8 LP assemblies were 59 ± 3, 119 ± 1,

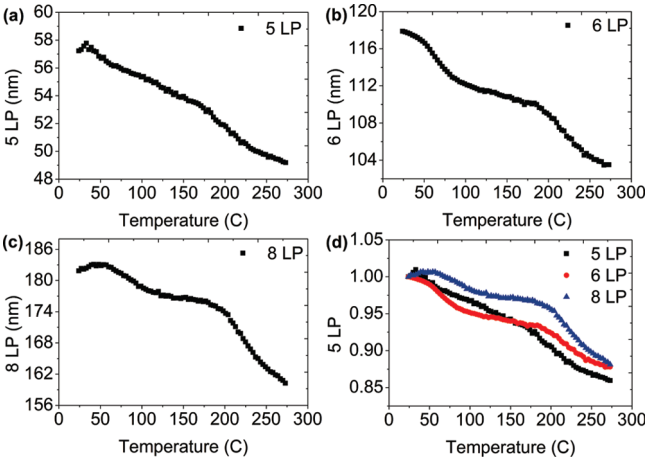

Figure 2. Film thickness of (a) 5 LP, (b) 6 LP, and (c) 8 LP dry PAH/PAA LbL assemblies measured using ellipsometry at varying temperatures. (d) Normalized thickness as a function of temperature.

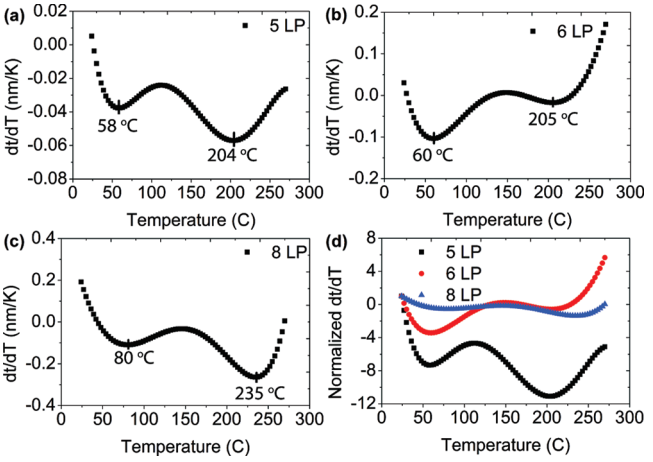

Figure 3. dt/dT vs temperature graphs of (a) 5 LP, (b) 6 LP, and (c) 8 LP PAH/PAA LbL films. (d) Normalized dt/dT vs temperature graph for 5, 6, and 8 LP.

and 183 ± 2 nm, respectively. Samples were heated from room temperature to 270 °C at a rate of 3 °C/min. Overall, film thickness decreased with increasing sample temperature, and two sharp declines in thickness, each around 50−100 and 200−250 °C, were present. Modest increases in film thickness were observed just above room temperature, possibly from thermal expansion or absorption of ambient water. The average thickness of 5, 6, and 8 LP PAH/PAA LbL assemblies declined by 14 ± 1, 12.18 ± 0.01, and 9 ± 4%, respectively, when heated from room temperature to 270 °C. Upon cooling from 270 °C to room temperature, film thickness changed negligibly. For ease of comparison, film thickness was normalized to each film's initial room temperature dry thickness, and the results are plotted together in Figure 2d.

Whereas a neutral polymer, such as polystyrene (PS), expands with increasing temperature owing to thermal expansion,[29,35] the layer-by-layer assembly contracts. The decrease in film thickness with increasing temperature may be attributed to a loss of mass and/or an increase in film density, where thermal expansion may be minor in comparison. Prior work on 200 LP PAH/PAA LbL films indicates that both anhydride formation and amidation occur upon heating, each of which evolve water and covalently cross-link the LbL matrix.[42] Therefore, it is reasonable to assume the reduction in LbL film thickness is a result of anhydride formation and amidation.

By taking the derivative of film thickness with respect to temperature, the declines in film thickness can be visualized more clearly. Figure 3 shows the first derivative of polynomials fit to 5, 6, and 8 LP PAH/PAA LbL assembly thickness profiles from Figure 2. Regardless of film's initial thickness or number of layer pairs, two minima were observed. The low-temperature minimum is attributed to anhydride formation, and the second minimum is attributed to amidation. The 5 and 6 LP samples experienced similar anhydration temperatures, whereas the 8 LP sample had a distinctively higher anhydration temperature. However, the average temperature of amidation steadily increased with increasing number of layer pairs (from 207 ± 5 °C for 5 LP to 240 ± 8 °C for 8 LP). For ease of comparison, each derivative was normalized by the film's initial room temperature thickness, and the results are plotted together in Figure 3d. The average temperature minima are summarized in Figure 4.

Given that ellipsometry measurements indicate that amidation temperature is influenced by film thickness, we sought to determine the origin of the relationship. One hypothesis is that hydroxyl groups on the native oxide surface catalyze the amidation reaction within thin PAH/PAA LbL films. As film thickness

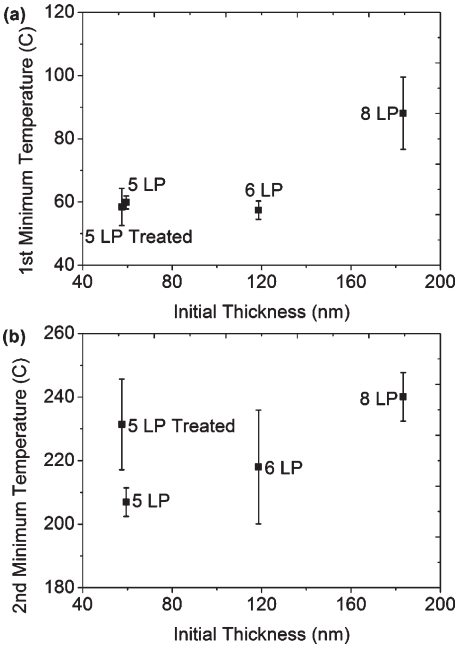

Figure 4. (a) First minimum temperature vs initial thickness. (b) Second minimum temperature vs initial thickness. Minimum temperatures were determined from derivatives of ellipsometry profiles indicated in Figure 3. Samples grown on HMDS-modified silicon are labeled "5 LP Treated". All other samples were grown on silicon wafers with native oxide. Data are plotted with respect to initial thickness, and the number of layer pairs corresponding to that thickness is labeled. Individual data points represent multiple measurements.

decreases, the amidation temperature may similarly decrease as the role of the catalytic supporting surface overtakes bulk behavior. To test this hypothesis, the surface of a silicon wafer was modified to have $-CH_3$ functionality using HMDS treatment. If the hydroxyl group was indeed catalytic, then modifying the surface to have $-CH_3$ functionality (thus, removing the catalyzing agent) should increase the amidation temperature.

The thickness of a 5LP PAH/PAA LbL film on HMDS-modified silicon was monitored using ellipsometry as before. Again, two sharp minima in the dt/dT curve were observed for the HMDS-treated samples; the temperatures of the two minimum dt/dT values were taken as the cross-linking temperature and are shown in Figure 4 ("5LP Treated"). Whereas HMDS surface treatment does not appreciably change the temperature of

anhydration (~58 °C, Figure 4a), HMDS surface treatment does have a profound influence on the temperature of amidation (231 ± 14 °C for HMDS-treated and 207 ± 5 °C for no treatment, Figure 4b). The large temperature difference supports the hypothesis that hydroxyl groups on the native oxide surface catalyze amidation within the LbL assembly. The same conclusion cannot be drawn for anhydration, where results were less clear.

To complement findings from ellipsometry, DSC was performed on LbL-coated porous AAO membranes. Both aluminum oxide and silicon oxide possess similar surface chemistry (i.e., hydroxyl groups),[47,48] so findings from films grown on either substrate are considered comparable. The advantage of using porous AAO membranes as substrates, rather than nonporous silicon wafer, is that the membrane's large surface area allows for a greater mass of LbL film to be deposited. Consequently, LbL-coated AAO membranes have adequate sample mass to yield useful results from DSC. Figure 5a shows a representative DSC thermogram for a 5 LP PAH/PAA LbL-coated AAO membrane. In the first cycle, the sample was heated to 170 °C and then cooled, each at 5 °C/min. Upon heating in the first cycle, a single endothermic peak was observed. In the second cycle, the sample was heated to 300 °C and cooled, each at 5 °C/min. Upon heating in the second cycle, a separate endothermic peak was also observed. Considering that neither peak appeared during cooling or subsequent cycles, the observed thermal events are considered irreversible. Prior work on DSC of bulk PAH/PAA LbL films suggests that the first and second peaks are attributed to anhydration and amidation, respectively.[42] As a control, a DSC thermogram of an uncoated AAO membrane had no significant thermal events; therefore, the events observed in Figure 5 are attributed solely to the LbL film.

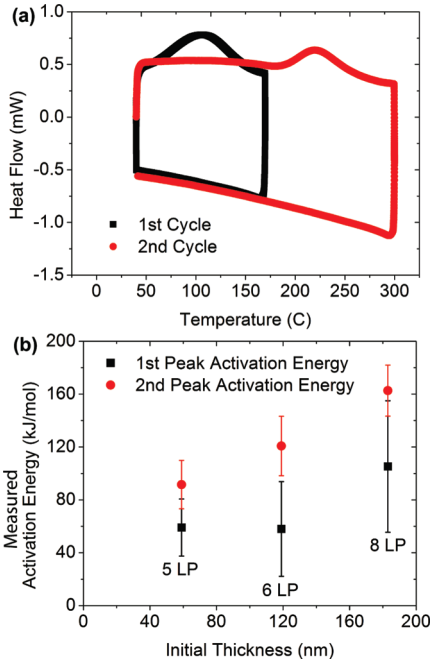

Figure 5. (a) A representative DSC thermogram for a 5 LP PAH/PAA LbL-coated AAO membrane with 5 °C/min heating and cooling rate. (b) Measured activation energies of 5, 6, and 8 LP samples. The first and second peaks are attributed to anhydride formation and amidation, respectively.

From ellipsometry experiments, it is clear that amidation temperature decreased with decreasing film thickness, whereas anhydration was not clearly influenced. Supposing that amidation is catalyzed by the substrate, the activation energy of the amidation reaction should decrease with decreasing film thickness as the influence of the substrate becomes more pronounced. To test this hypothesis, the activation energy, E_a, of both reactions within LbL films of varying thicknesses was determined using the Ozawa method.[49] The scan rate, a, is related to the peak absolute temperature, T_m, via

$$\log a = -\frac{0.4567E_a}{RT_m} - 2.315 + \log\frac{AE_a}{R} - \log G(x_m) \qquad (1)$$

where R is the universal gas constant, A is a pre-exponential factor associated with the Arrhenius equation, and $G(x_m)$ is a constant (assuming isoconversion). According to eq 1, log a vs T_m^{-1} should yield a line with slope $-0.4567E_a/R$.[49] To determine the measured activation energy of the reactions, DSC was performed at multiple scan rates for 5, 6, and 8 LP, and data are summarized in Table 1. Figure 5b shows the calculated activation energies of the first and second peaks for films of varying initial thickness (i.e., number of layer pairs). LbL film thickness on an AAO membrane was assumed to be similar to that measured via ellipsometry on silicon wafer. The measured activation energy of the second peak (amidation) decreased with decreasing thickness, confirming the hypothesis that amidation is catalyzed or accelerated within thinner films. In contrast, error within the measured activation energy from the first peak (anhydride formation) was too large to draw any conclusions.

Both anhydride and amide reactions yield water as a byproduct, so the mass of the LbL film should decrease during both reactions. TGA was performed on 5, 6, and 8 LP PAH/PAA LbL assemblies on AAO membranes to determine the amount of mass lost during heating. Figure 6a shows a representative TGA thermogram of a 5 LP LbL-coated AAO membrane. Identical to the temperature program implemented by DSC, an LbL-coated membrane was subjected to two heating and cooling cycles. First, the sample was heated to 170 °C from room temperature at 3 °C/min, held isothermally, and then cooled back to room temperature. Then the sample was heated to 300 °C at that same rate. The axes in Figure 6a,b are shown in units of time rather than temperature because changes in mass corresponding with the isothermal step are more clearly visible. The TGA thermogram (Figure 6a) of LbL assembly has two distinct weight loss regions, similar to a previous report on the analogous bulk system.[42] There was a 0.9 wt % loss from 2 to 46 min (46 to 165 °C) and a 1.3 wt % weight loss from 140 to 180 min (180 to 200 °C). The low-temperature weight-loss region is attributed to

Table 1. Summary of Reaction Temperatures with Varying Scan Rates and Varying Number of PAH/PAA Layer Pairs Measured Using Ellipsometry, TGA, and DSC

		anhydride temperature (°C)				amidation temperature (°C)			
	scan rate (°C/min)	5 LP	6 LP	8 LP	200 LP[b]	5 LP	6 LP	8 LP	200 LP[b]
ellipsometry	3	60 ± 2 (56 ± 6)[a]	57 ± 3	88 ± 11		207 ± 5 (231 ± 14)[a]	218 ± 8	240 ± 8	
TGA	3	46−165	48−170	46−99	40−150	204	208	214	250
DSC	3	92	98	101	102	205	217	223	251
	5	107	115	111		220	228	231	
	10	112	116	113		230	236	238	

[a] Reaction temperatures from HMDS-modified silicon wafer. [b] Data taken from Shao and Lutkenhaus.[42]

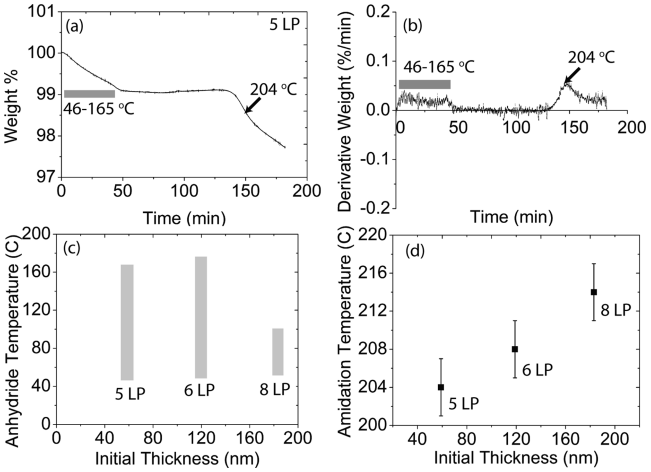

Figure 6. (a) TGA thermogram of representative 5 LP PAH/PAA LbL assemblies on AAO membranes. (b) Derivative weight vs time of representative 5 LP PAH/PAA LbL assemblies on AAO membranes. (c) The range of the anhydration peak temperature vs initial thickness for 5, 6, and 8 LP samples. (d) Amidation temperature vs initial thickness for 5, 6, and 8 LP samples.

desorption of loosely bound water and water evolved from anhydride formation. The higher temperature weight-loss region is attributed to water evolved from amidation. The mass lost during heating is small because the AAO membrane accounts for the majority of the sample mass. Figure 6b is derivative weight vs time of the representative 5 LP system in Figure 6a. The signal from the anhydration reaction was broad and difficult to pinpoint, so the anhydration temperature was described as the temperature range depicted in the shaded bars in Figure 6c. In contrast, the temperature of amidation was clear and taken as the peak in the weight derivative curve. Amidation temperature increased with increasing initial film thickness (Figure 6d), similar to observations from ellipsometry and DSC. Results are summarized in Table 1.

Discussion

The preceding results for PAH/PAA LbL assemblies, summarized in Table 1, collectively indicate that amidation temperature is strongly dependent on film thickness and substrate chemistry. Ellipsometry is not commonly used to monitor cross-linking kinetics within LbL assemblies, and the data herein demonstrate that it is a useful technique for accessing thermochemical information within ultrathin LbL films. From ellipsometry, it is clear that amidation temperature decreases as LbL film thickness decreases (Figure 7a); trends from DSC and TGA both match this observation. The origin of this "confinement effect" was hypothesized to be related to the catalytic contribution of the substrate, which becomes more obvious in thinner films. Both silicon with native oxide and aluminum oxide membranes have similar influence on amidation, possibly because of their similar surface chemistry (i.e., hydroxyl groups). In contrast, LbL films on HMDS-treated silicon (bearing $-CH_3$ surface chemistry) had amidation temperatures characteristic of thicker films; in other words, replacement of the hydroxyl surface groups with HMDS removed or suppressed the supposed confinement effect (Figure 7b). Indeed, as indicated by Yang et al., silica gel is an effective medium in catalyzing amidation.[50]

The evidence of accelerated amidation within PAH/PAA LbL thin films is also supported by trends in the measured activation energy observed using DSC. The measured activation energy of amidation decreased with decreasing film thickness (Figure 5b), reflecting that the activation barrier for amide formation is lower in thinner films. Elsewhere, the activation energy for bulk

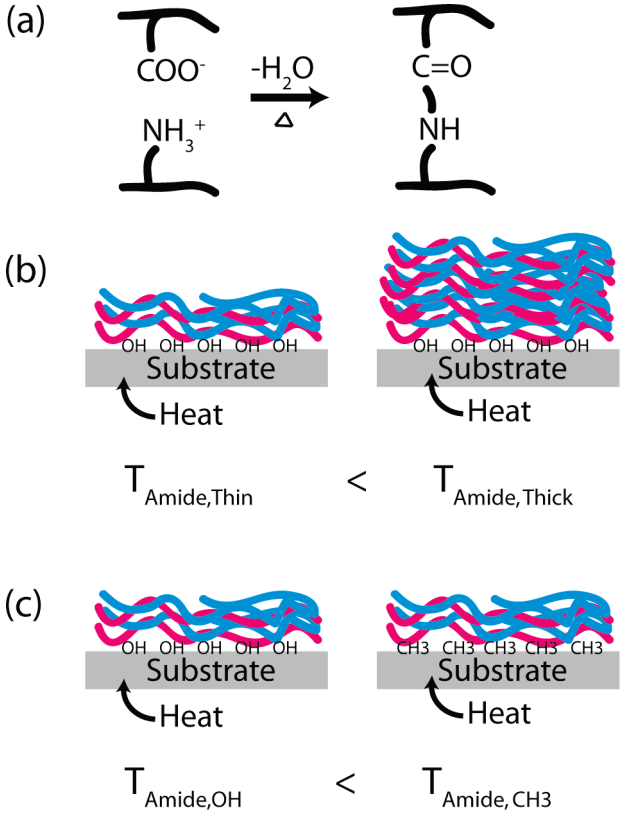

Figure 7. (a) Covalent amide bonding of PAH/PAA LbL assemblies. (b) The curing (amidation) temperature of the thin confined LbL film is lower than that of the thick, bulk LbL film. (c) The curing temperature of film atop a native oxide surface is lower than that of the HMDS-modified surface.

polyamide synthesis at low conversion was 155 kJ/mol, which was similar to that reported here for a 183 nm thick 8 LP film (~160 kJ/mol).[51] Even so, this similarity does not reflect that an 8 LP PAH/PAA film may be regarded as a bulk material because the amidation temperature for an 8 LP film (223 °C) was considerably lower than that of a 200 LP film (251 °C) (Table 1).

Amide cross-linking within PAH/PAA LbL films has been reported elsewhere by others,[41,52−54] where temperatures ranging from 130 to 350 °C were employed. Substrates used ranged from gold-coated silicon wafer to ITO and polysulfone membranes. Results presented herein support that amide curing or cross-linking is applicable at such temperatures and suggest that the degree of cross-linking (i.e., whether a film is "lightly" or "heavily" cross-linked) may be controlled by selecting an appropriate cross-linking temperature and time. Although others cross-link films at temperatures well below the amidation temperature values indicated here, it is reasonable that amidation may occur at lower temperatures if the onset temperature is considered. Here, the onset temperatures of amidation for 5, 6, and 8 LP PAH/PAA LbL films were 162, 166, and 177 °C, respectively. The rate of amidation (i.e., the rate of cross-links formed) may be controlled by adjusting the temperature because the reaction rate coefficient, k, scales with temperature via $k = Ae^{-E_a/RT}$. Therefore, increasing the temperature is expected to increase the rate of amide bonds forming and vice versa.

In contrast, the anhydration temperature did not have a clear dependence on film thickness. One possible reason includes the error introduced by ambient water. Extreme care was taken to thoroughly dry each sample prior to testing (e.g., vacuum overnight, prolonged nitrogen purge in DSC and TGA), but opportunity for water contamination was still possible. Water can potentially have a strong influence on data from ellipsometry

because experiments were conducted in ambient air. Absorbed water may broaden features near and below 100 °C as absorbed water leaves the film. Above 100 °C, water did not have a strong influence, and data obtained at higher temperatures were reliable and reproducible. Anhydride functional groups can also participate in amidation, where an anhydride reacts with an amine to form an amide. This pathway is plausible considering that anhydride peaks disappears from IR spectra for samples heated from 100 to 250 °C.[42]

Another issue to consider is whether the internal architecture of the film itself evolves with successive cycles of LbL deposition. The PAH/PAA system grows linearly (at PAH pH = 7.5 and at PAA pH = 3.5), and its modulus is invariant with film thickness.[55] Additionally, even a single layer pair of the PAH/PAA system was sufficient to significantly alter a substrate's water contact angle.[56] In a separate study, water contact angle reached a steady value for four layer pairs and higher of PAH/PAA (pH 7.5/3.5).[57] Together, these reports suggest that even in the thickness range investigated presently (5−8 LP) the films' internal architecture may be assumed to be uniform from sample to sample.

As was previously mentioned, curing within thermosetting resins under nanoscale constraint has been recently explored, and findings highlight other possible mechanisms behind the influence of confinement on the amidation temperature within PAH/PAA LbL films. For bisphenol M dicyanate ester within a controlled pore glass, the rate of cure increased as the size of the pore decreased.[31,38,39] Hydroxyl groups within the pore were shown to accelerate curing, but controlled studies indicated that surface chemistry was not solely responsible for the acceleration; a less mobile layer confined near the pore wall was proposed to have increased collision frequency, contributing to the curing process.[39] Similarly, our results indicate that surface chemistry catalyzes amidation, but other contributions, such as a confined surface layer, may also play a role.

Conclusion

The effect of confinement on cross-linking within electrostatic LbL assemblies was studied using ellipsometry, DSC, and TGA. Using temperature-controlled ellipsometry, cross-linking within PAH/PAA LbL films was monitored via changes in film thickness. Amidation temperature decreased when film thickness was decreased, indicating an acceleration of the cross-linking reaction. In contrast, the influence of thickness on anhydride formation was unclear. The accelerated amidation reaction was attributed to the catalytic activity of the supporting substrate, as evidenced by an increased amidation temperature for an alternate substrate surface chemistry (i.e., HMDS). The catalytic influence of the substrate was more apparent in thinner films, where the measured activation energy of the reaction decreased with decreasing film thickness. Our work provides a new insight into understanding the effect of confinement on ultrathin LbL assemblies and suggests that the substrate can play a significant role in some instances.

Temperature-controlled ellipsometric analysis and thermal analysis of ultrathin layer-by-layer films can potentially yield a wealth of information regarding whether LbL films have unique cross-linking kinetics; whether they have none, one, or multiple glass transitions; or whether confinement influences those thermochemical properties. For example, ongoing work in our laboratory indicates that temperature-controlled ellipsometry can be used to detect glass transitions within ultrathin LbL films and will be reported elsewhere. Future work will target LbL films containing different combinations of weak and strong polyelectrolytes, systems that grow linearly or exponentially, and films containing nanoparticles.

Acknowledgment. J. L. Lutkenhaus thanks Yale University and Texas A&M University setup funds.

Supporting Information Available: Sample's surface temperature calculation. This material is available free of charge via the Internet at http://pubs.acs.org.

References and Notes

(1) Su, X. F.; Kim, B. S.; Kim, S. R.; Hammond, P. T.; Irvine, D. J. *ACS Nano* **2009**, *3*, 3719.
(2) Schneider, G. F.; Subr, V.; Ulbrich, K.; Decher, G. *Nano Lett.* **2009**, *9*, 636.
(3) Sexton, A.; Whitney, P. G.; Chong, S. F.; Zelikin, A. N.; Johnston, A. P. R.; De Rose, R.; Brooks, A. G.; Caruso, F.; Kent, S. J. *ACS Nano* **2009**, *3*, 3391.
(4) Yan, Y.; Johnston, A. P. R.; Dodds, S. J.; Kamphuis, M. M. J.; Ferguson, C.; Parton, R. G.; Nice, E. C.; Heath, J. K.; Caruso, F. *ACS Nano* **2010**, *4*, 2928.
(5) Wong, S. Y.; Li, Q.; Veselinovic, J.; Kim, B. S.; Klibanov, A. M.; Hammond, P. T. *Biomaterials* **2010**, *31*, 4079.
(6) Quinn, A.; Such, G. K.; Quinn, J. F.; Caruso, F. *Adv. Funct. Mater.* **2008**, *18*, 17.
(7) Zhou, J.; Romero, G.; Rojas, E.; Ma, L.; Moya, S.; Gao, C. Y. *J. Colloid Interface Sci.* **2010**, *345*, 241.
(8) Jang, W. S.; Saito, T.; Hickner, M. A.; Lutkenhaus, J. L. *Macromol. Rapid Commun.* **2010**, *31*, 745.
(9) Lutkenhaus, J. L.; Hrabak, K. D.; McEnnis, K.; Hammond, P. T. *J. Am. Chem. Soc.* **2005**, *127*, 17228.
(10) Lutkenhaus, J. L.; McEnnis, K.; Hammond, P. T. *Macromolecules* **2007**, *40*, 8367.
(11) Farhat, T. R.; Hammond, P. T. *Chem. Mater.* **2006**, *18*, 41.
(12) Argun, A. A.; Ashcraft, J. N.; Hammond, P. T. *Adv. Mater.* **2008**, *20*, 1539.
(13) Abebe, D. G.; Farhat, T. R. *Soft Matter* **2010**, *6*, 1325.
(14) Nam, K. T.; Kim, D. W.; Yoo, P. J.; Chiang, C. Y.; Meethong, N.; Hammond, P. T.; Chiang, Y. M.; Belcher, A. M. *Science* **2006**, *312*, 885.
(15) Nam, K. T.; Wartena, R.; Yoo, P. J.; Liau, F. W.; Lee, Y. J.; Chiang, Y. M.; Hammond, P. T.; Belcher, A. M. *Proc. Natl. Acad. Sci. U.S.A.* **2008**, *105*, 17227.
(16) Benten, H.; Ogawa, M.; Ohkita, H.; Ito, S. *Adv. Funct. Mater.* **2008**, *18*, 1563.
(17) Luther, J. M.; Law, M.; Beard, M. C.; Song, Q.; Reese, M. O.; Ellingson, R. J.; Nozik, A. J. *Nano Lett.* **2008**, *8*, 3488.
(18) Liu, Y.; Cui, T. H. *Sens. Actuators, B* **2007**, *123*, 148.
(19) Xue, W.; Cui, T. H. *Sens. Actuators, B* **2008**, *134*, 981.
(20) Hua, F.; Shi, J.; Lvov, Y.; Cui, T. *Nanotechnology* **2003**, *14*, 453.
(21) DeRocher, J. P.; Mao, P.; Han, J. Y.; Rubner, M. F.; Cohen, R. E. *Macromolecules* **2010**, *43*, 2430.
(22) Decher, G.; Hong, J. D.; Schmitt, J. *Thin Solid Films* **1992**, *210*, 831.
(23) Decher, G. *Science* **1997**, *277*, 1232.
(24) Stockton, W. B.; Rubner, M. F. *Macromolecules* **1997**, *30*, 2717.
(25) Cerda, J. J.; Qiao, B.; Holm, C. *Soft Matter* **2009**, *5*, 4412.
(26) Alcoutlabi, M.; McKenna, G. B. *J. Phys.: Condens. Matter* **2005**, *17*, R461.
(27) Barrat, J. L.; Baschnagel, J.; Lyulin, A. *Soft Matter* **2010**, *6*, 3430.
(28) Binder, K.; Horbach, J.; Vink, R.; De Virgiliis, A. *Soft Matter* **2008**, *4*, 1555.
(29) Keddie, J. L.; Jones, R. A. L.; Cory, R. A. *Europhys. Lett.* **1994**, *27*, 59.
(30) Weimann, P. A.; Hajduk, D. A.; Chu, C.; Chaffin, K. A.; Brodil, J. C.; Bates, F. S. *J. Polym. Sci., Part B: Polym. Phys.* **1999**, *37*, 2053.
(31) Li, Q. X.; Simon, S. L. *Macromolecules* **2008**, *41*, 1310.
(32) Frank, C. W.; Rao, V.; Despotopoulou, M. M.; Pease, R. F. W.; Hinsberg, W. D.; Miller, R. D.; Rabolt, J. F. *Science* **1996**, *273*, 912.
(33) Xu, S. H.; O'Connell, P. A.; McKenna, G. B. *J. Chem. Phys.* **2010**, *132*, 184902.
(34) Keddie, J. L.; Jones, R. A. L.; Cory, R. A. *Europhys. Lett.* **1994**, *27*, 59.
(35) Kim, S.; Hewlett, S. A.; Roth, C. B.; Torkelson, J. M. *Eur. Phys. J. E* **2009**, *30*, 83.
(36) Serghei, A.; Huth, H.; Schick, C.; Kremer, F. *Macromolecules* **2008**, *41*, 3636.
(37) Liu, Y.; Russell, T. P.; Samant, M. G.; Stohr, J.; Brown, H. R.; Cossy-Favre, A.; Diaz, J. *Macromolecules* **1997**, *30*, 7768.

(38) Koh, Y. R.; Li, Q. X.; Simon, S. L. *Thermochim. Acta* **2009**, *492*, 45.
(39) Li, Q. X.; Simon, S. L. *Macromolecules* **2009**, *42*, 3573.
(40) Amanuel, S.; Malhotra, V. M. *J. Appl. Polym. Sci.* **2006**, *99*, 3183.
(41) Harris, J. J.; DeRose, P. M.; Bruening, M. L. *J. Am. Chem. Soc.* **1999**, *121*, 1978.
(42) Shao, L.; Lutkenhaus, J. L. *Soft Matter* **2010**, *6*, 3363.
(43) Shiratori, S.; Rubner, M. F. *Macromolecules* **2000**, *33*, 4213.
(44) Jackson, C. L.; McKenna, G. B. *J. Chem. Phys.* **1990**, *93*, 9002.
(45) Dubinsky, S.; Grader, G. S.; Shter, G. E.; Silverstein, M. S. *Polym. Degrad. Stab.* **2004**, *86*, 171.
(46) Dragan, E. S.; Mihai, M.; Airinei, A. *J. Polym. Sci., Polym. Chem.* **2006**, *44*, 5898.
(47) Qi, F.; Xu, B.; Chen, Z.; Ma, J.; Sun, D.; Zhang, L. *Sep. Purif. Technol.* **2009**, *66*, 405.
(48) Weldon, M. K.; Chabal, Y. J.; Hamann, D. R.; Christman, S. B.; Chaban, E. E.; Feldman, L. C. *J. Vac. Sci. Technol. B* **1996**, *14*, 3095.
(49) Ozawa, T. *J. Therm. Anal. Calorim.* **1970**, *2*, 301.
(50) Yang, X.-D.; Zeng, X.-H.; Zhao, Y.-H.; Wang, X.-Q.; Pan, Z.-Q.; Li, L.; Zhang, H.-B. *J. Comb. Chem.* **2010**, *12*, 307.
(51) Khan, A. R.; Al-Roomi, Y. M.; Mathew, J.; Sari, M. *J. Appl. Polym. Sci.* **2001**, *82*, 2534.
(52) Mendelsohn, J. D.; Barrett, C. J.; Chan, V. V.; Pal, A. J.; Mayes, A. M.; Rubner, M. F. *Langmuir* **2000**, *16*, 5017.
(53) Zhai, L.; Cebeci, F. C.; Cohen, R. E.; Rubner, M. F. *Nano Lett.* **2004**, *4*, 1349.
(54) Park, J.; Park, J.; Kim, S. H.; Cho, J.; Bang, J. *J. Mater. Chem.* **2010**, *20*, 2085.
(55) Nolte, A. J.; Cohen, R. E.; Rubner, M. F. *Macromolecules* **2006**, *39*, 4841.
(56) Yoo, D.; Shiratori, S. S.; Rubner, M. F. *Macromolecules* **1998**, *31*, 4309.
(57) Fujita, S.; Shiratori, S. *Nanotechnology* **2005**, *16*, 1821.